

## Effect of Alloyed Mo and W on The Corrosion Characteristics of Super Duplex Stainless Steel Weld

Hae-Ji Park, Hae-Woo Lee\*

Department of Materials Science and Engineering, Dong-A University, 840 Hadan-dong, Saha-gu, Busan 604-714, Republic of Korea

\*E-mail: [hwlee@dau.ac.kr](mailto:hwlee@dau.ac.kr)

Received: 14 July 2014 / Accepted: 5 September 2014 / Published: 29 September 2014

---

The corrosion behavior of super duplex stainless steel (SDSS) weldments which depend on Mo and W content has been studied. In order to compare the electrochemical characteristics depending on the change in the content of Mo and W, Anodic Polarization Tests were conducted in the 3.5%NaCl solution and 1M H<sub>2</sub>SO<sub>4</sub> solution before observing the changes in the microstructure. The observation results of the microstructure showed that the fraction of  $\delta$ -ferrite increased as Mo was partially substituted by W, and  $\gamma$  grew with a constant directional property. Also, the analysis results of the phase after aging the specimens for 30 minutes at 800 °C showed that there was less  $\sigma$  phase precipitation in the W added specimen than that of only Mo added. Though the results of potentiodynamic polarization test showed no difference in corrosion resistance in as-weld state, in the polarization test after aging treatment, the W added specimen showed superior corrosion resistance to that of only Mo added. As a result of analyzing the microstructure after the polarization test, pitting occurred in a Cr and Mo depleted zone around  $\sigma$  phase.

---

**Keywords:** Super Duplex Stainless Steels; Molybdenum; Tungsten; Welding; Corrosion; Pitting

### 1. INTRODUCTION

As nuclear and chemical industries have advanced, the demand for duplex stainless steel (DSS), which is used as structural material for such industries, increases. Austenite ( $\gamma$ ) and ferrite ( $\delta$ ) exist concurrently in DSS, while they are independently exist in the existing stainless steel. Furthermore, corrosion resistance and weldability of DSS are superior to those of the existing stainless steel [1].

Today, with advancement in industrial technologies, materials which can be used under more severe corrosive environment have been demanded, and one of such materials is Super Duplex

Stainless Steel (SDSS). As SDSS has a Pitting Resistance Equivalent Number (PREN) of 40 or bigger, it exhibits superior corrosion resistance not only in petrochemical or chemical plant industries but also in chloride environment and its overall properties are more superior to those of the existing DSS. However, SDSS has a disadvantage that it has many restrictions in high temperature processes such as hot working or welding because diverse precipitate phases are easily generated during manufacture and heat treatment and it contains much alloy elements in comparison to other steel grades.

It has been known that the addition of Mo improves corrosion resistance greatly, especially against pitting and stress corrosion in a solution of chloride environment [2 and 3]. However, as the addition of Mo increases, formation of the vulnerable secondary phases such as sigma ( $\sigma$ ) and chi ( $\chi$ ) phases are promoted in the alloy when it is exposed to high temperature between 600 and 900 °C [4 and 5]. In particular,  $\sigma$  phase is a very vulnerable compound of metals, which aggravates impact toughness and corrosion resistance of materials when only about 1 vol% is generated [6 and 7].

Accordingly, many DSS studies have been conducted on suppression of the second precipitate phases [8 and 9], and, as a result, studies are being conducted on partial substitution of Mo with W (tungsten) which belongs to the same family in the periodic table of the elements and has physical and chemical properties similar to those of Mo.

According to the findings of studies known up to now, W added in place of Mo is known to suppress formation of  $\sigma$  phase without reducing the corrosion resistance of DSS [10, 11 and 12]. Also, the synergy effect of Mo and W is reported. Belfrouh *et al.* reported that the passivation speed of the steel to which Mo and W are added is shown to be faster than that of the steel to which only Mo is added [13].

The corrosion resistance improvement mechanism of W is proposed to increase in the interfacial adhesion between metals and oxides or prevent invasion of anions and fluidity of cations achieved by forming tungsten oxide (WO<sub>3</sub>) or Tungstate (WO<sub>4</sub><sup>2-</sup>) depending on the environment [7].

The corrosion resistance of SDSS weld deteriorates due to changes in the  $\gamma/\delta$  fraction and formation of the precipitate phases caused by rapid heating and cooling during welding. While studies have been conducted before on formation of the secondary phases in the alloys of which Mo are partially substituted with W and the resulting change in mechanical properties, studies on the effect of partial substitution of Mo with W under an environment accompanying severe thermal change, such as welding on corrosion resistance, is not yet sufficient.

In this study, Flux Cored Arc Welding (FCAW) was conducted to produce two types of welding materials of which the contents of Mo and W were changed based on Fe-25Cr-9Ni-0.15N alloy. After that, the improvement effect of substitution of Mo element with W on corrosion resistance of deposited metal was investigated through a Potentiodynamic Polarization Test. Also, the electrochemical change was observed along with the change in the microstructure caused by local corrosion using a SEM-EDS (JSM-9400F, Jeol, Japan) and Electron Back Scattering Diffraction (EBSD).

## 2. EXPERIMENTAL PROCEDURE

### 2.1. Welding Material and Method

As to welding, FCAW was conducted in the condition two SUS304 steel materials produced in a size of 290 mm x 140 mm x 20 mm (thickness) are placed butting each other. As to welding wires, two types were produced by adding 3 % of Mo and 2.2 % of Mo plus 2.2 % of W together respectively to the basic composition of Fe-25Cr-9Ni-0.15N. The chemical composition of the deposited metals was measured using Optical Emission Spectrometer (Metal-Lab75/80J, GNR srl, Italy), of which the values are shown in Table 1. The root gap used was 10 mm and the groove angle was 45° as shown in Figure 1. Welding was conducted using 99.9 % CO<sub>2</sub> at the rate of 25 l/min as the shielding gas and DCRP(+). The welding conditions are shown in Table 2.

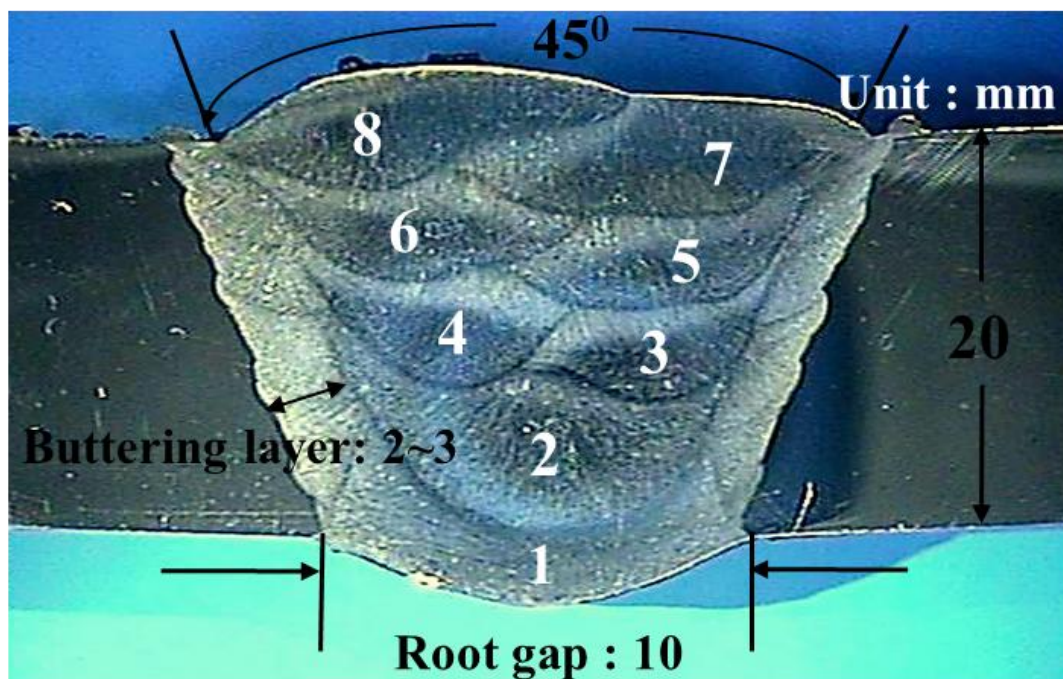


Figure 1. Schematic Diagram of Weld Specimen

Table 1. Chemical Composition of the Weld Metals (wt%)

	C	N	Si	Mn	P	S	Cr	Ni	Mo	W	PREN30
3Mo	0.03	0.15	0.41	0.81	0.01	0.03	25.38	9.73	3.09	-	40.07
2.2Mo- 2.2W	0.03	0.15	0.44	0.82	0.01	0.03	25.18	9.75	2.21	2.24	40.66

**Table 2.** Welding Condition

Test No.	Current (A)	Voltage (V)	Interpass temperature (°C)	Travel Speed (CPM)	Heat input (KJ/mm)	Layers
3Mo	180	29	22	14.03	2.23	1
	220	32	77	14.15	2.99	2
	220	32	124	24.86	1.70	3
	220	32	130	25.59	1.65	3
	220	32	139	20.96	2.01	4
	220	32	120	21.22	1.99	4
	220	32	144	21.75	1.94	5
	220	32	141	25.97	1.63	5
2.2Mo-2.2W	180	28	8	13.66	2.21	1
	220	32	106	15.12	2.79	2
	220	32	144	32.11	1.32	3
	220	32	128	29.05	1.45	3
	220	32	135	24.40	1.73	4
	220	32	127	23.46	1.80	4
	220	32	126	24.08	1.75	5
	220	32	138	26.52	1.59	5

## 2.2. Observation of Microstructure and Phase Analysis

In order to observe the microstructure and precipitate phases of the deposited metal, the condition of  $\sigma$  precipitation was observed using a SEM-EDS after grinding, polishing and electrolytic etching in 20 % KOH solution. Also, EBSD method was used to analyze the secondary precipitate phases and the residual phases.

## 2.3. Measurement of Ferrite Content

The contents of  $\delta$ -ferrite remaining in the welding materials (3Mo and 2.2Mo-2.2W) were measured by welding pass using a Ferrite Scope (MP30E-S, Fischer, Germany), and the mean value is shown as the Ferrite Content (wt%).

## 2.4. Measurement of Nitrogen

In order to measure the nitrogen content in each specimen, a nitrogen analyzer (ELTRA GmbH, ELTRA Oxygen/Nitrogen Determinator ON-900) was used.

## 2.5. Aging Treatment

In order to observe the precipitation conditions of  $\sigma$  and  $\chi$  phases depending on the aging temperature, aging treatment was conducted for 30 minutes at 800 °C using a vacuum heat treatment furnace before conducting water cooling.

2.6. Potentiodynamic Polarization Test

In order to compare the electrochemical properties which change in accordance with Mo and W contents, anodic polarization tests were conducted in 3.5%NaCl solution and 1M H<sub>2</sub>SO<sub>4</sub> Solution. The range of electrode potential was set to -1 V to 1.5 V, and the scanning speed to 0.4 V/s. The working electrode of the anodic polarization test was the specimen, the counter electrode was a platinum foil, and the reference electrode was an Ag-AgCl/KCl electrode. Also, the microstructure and the corrosion trend before and after the aging were compared after the polarization test using a SEM-EDS.

3. RESULTS AND DISCUSSION

3.1. Observation of Microstructure

Figure 2 shows the microstructure of two specimens, 3Mo and 2.2Mo-2.2W, after welding.  $\gamma$  phase is distributed over the matrix structure of  $\delta$ -ferrite. Table 3 shows the mean value obtained by measuring the content of  $\delta$ -ferrite using a Ferrite Scope. In the case of 3Mo specimen, the fraction of  $\delta$ -ferrite was measured to be 40 %, while it was 55 % in the case of 2.2Mo-2.2W. As Mo was partially substituted with W, these elements took the role of ferrite stabilization elements determining the fraction of  $\delta$ -ferrite. And, it can be observed that  $\gamma$  grows with a fixed directional property, and such interrelation between  $\delta$ -ferrite and the directional property of  $\gamma$  is known by Kudjumov-Sachs relationship ((110)bcc//((111)fcc, [0-11]bcc//[0-11]fcc) [14].

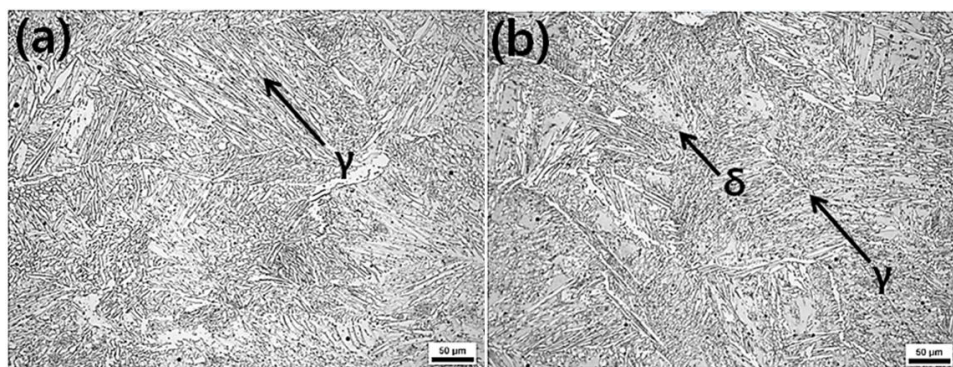
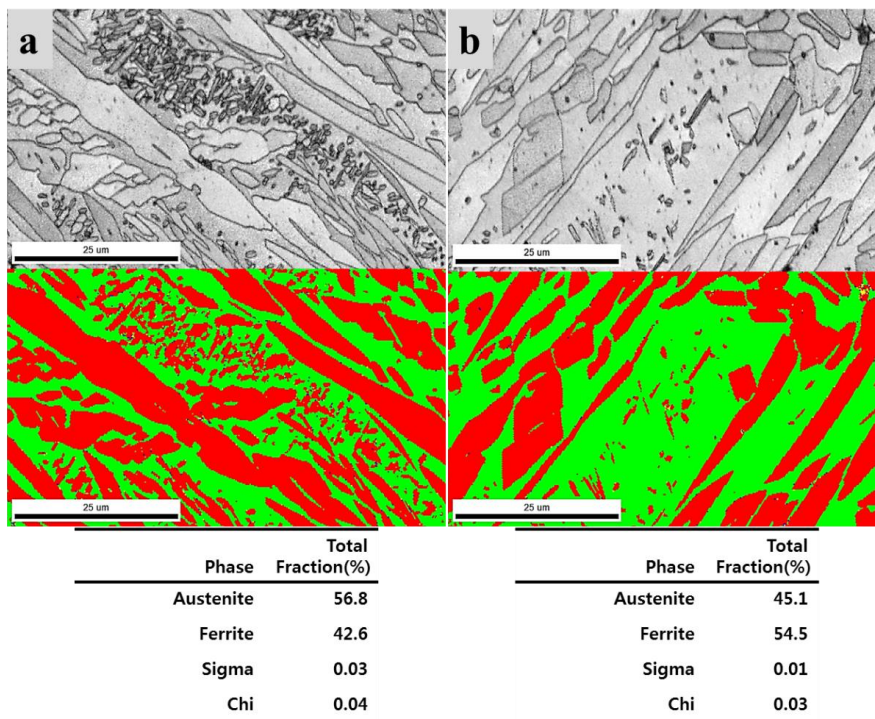


Figure 2. Optical Microstructure of Weld Metal showing Ferrite Phase (Gray Regions) and Austenitic Phase (White Regions): (a) 3Mo, (b) 2.2Mo-2.2W

Table 3. Delta-ferrite Contents (wt%) measured in Welds after Heat Treatment for 30 Minutes

	Delta-ferrite contents (wt%)	
	3Mo	2.2Mo-2.2W
As-weld	40	55
800 °C	4	11

Figure 3 shows the EBSD phase maps of (a) 3Mo-As weld and (b) 2.2Mo-2.2W-As weld specimens. Red color  $\gamma$  phase exists in the green color  $\delta$ -ferrite matrix, and, in the case of 3Mo specimen,  $\delta$ -ferrite was measured to be 42 % while it was 54.5 % in the case of 2.2Mo-2.2W specimen. Such a result largely corresponds with the  $\delta$ -ferrite content measured using a Ferrite Scope.



**Figure 3.** EBSD Phase Map. Color Scheme for Phase ID: Red- $\gamma$ -austenite, Green- $\delta$ -ferrite, Yellow-sigma Phase, and Blue-chi Phase: (a) 3Mo-As Weld (b) 2.2Mo-2.2W-As Weld

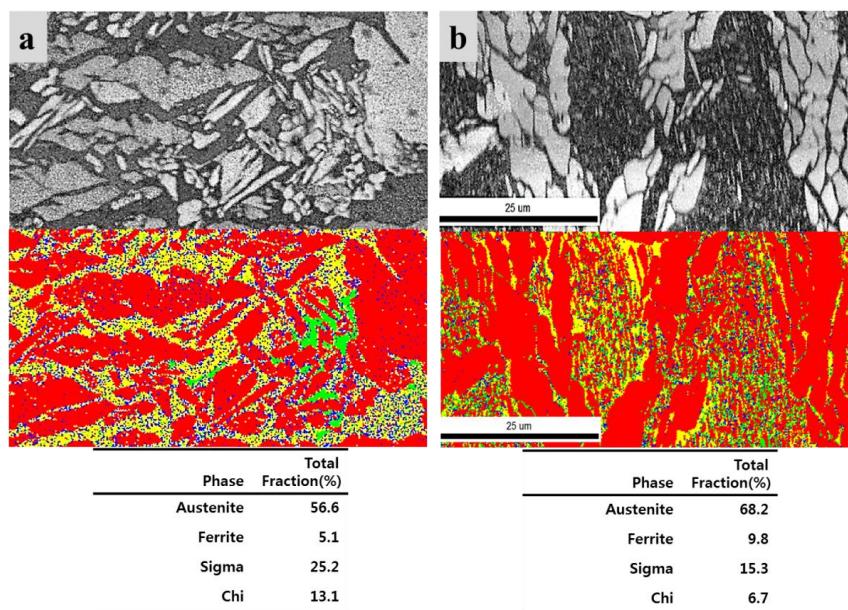


**Figure 4.** EBSD Phase Map. Color scheme for Phase ID: Red- $\gamma$ -austenite, Green- $\delta$ -ferrite, Yellow-sigma Phase, Blue-chi Phase: (a) 3Mo-800 (b) 2.2Mo-2.2W-800

Fig. 4 shows the EBSD phase map of the specimens (a) 3Mo-800 and (b) 2.2Mo-2.2W-800. As the action of  $\delta$  ferrite  $\rightarrow \sigma + \gamma_2$  was promoted and  $\delta$ -ferrite was metamorphosed into the secondary phase and  $\gamma_2$  by aging, the residual  $\delta$ -ferrite amount of 3Mo specimen which was 43.6 % before the aging was measured to be 5.1 wt%, and that of the 2.2Mo-2.2W specimen was also reduced from 54.5 % to 8.8 %. Also, under the same aging condition, the  $\sigma$  phase precipitation of the 2.2Mo-2.2W specimen was measured to be smaller than that of 3Mo specimen by about 12 %. Precipitation of secondary phase results from diffusion of an element such as W or Mo. The diffusion speed of W in iron or an iron-based alloy at 850 °C is known to be 1/10 to 1/100 that of Mo [15 and 16]. That is to say, as the diffusion speed of W is slow, it is not sufficiently diffused into  $\delta$ -ferrite and is piled up on the grain boundary plane promoting precipitation of  $\chi$  phase [17]. Therefore, in the case of 2.2Mo-2.2W specimen of which Mo is partially substituted with W, as  $\chi$  phase is continuously precipitated along the grain boundary plane, precipitation of  $\sigma$  phase is presumed to have been suppressed in comparison to the 3Mo specimen because Cr and Mo are relatively depleted.

Accordingly, if Mo is partially substituted with W, the local corrosion resistance of weld is presumed to be also reduced in the same condition as formation of  $\sigma$  phase is suppressed due to slow diffusion speed of W and stabilization of  $\chi$  phase.

### 3.2 Observation of Polarization Behavior

In order to study the anodic polarization behavior of SDSS weld appearing when Mo among alloy elements is partially substituted with W, potentiodynamic polarization tests were conducted in the aqueous solutions of 3.5%NaCl and 1M H<sub>2</sub>SO<sub>4</sub>.

Fig. 5(a) shows the polarization curves of the two specimens, 3Mo and 2.2Mo-2.2W, before the aging conducted in the aqueous solution of 3.5%NaCl. In as weld state, the corrosion potential values of the two specimens were -0.25 V (Ag/AgCl) and the pitting potential values of the two specimens were 1.1 V (Ag/AgCl) showing values similar to each other respectively, and their passive state areas were also very similar (to each other). Above the primary passive potential,  $E_{pp}$ , the passive film becomes stable, and corrosion rate falls to very low values in the passive state. Chromium is known to improve resistance of Fe-base alloy to general corrosion and local corrosion by forming oxidefilm. And, also, titanium, tantalum, and niobium form very stable insulating surface films which are resistant at very highly oxidizing potentials, leading to their use in anodes for impressed current cathodic protection systems. Meanwhile, in the case the test was conducted after aging treatment for 30 minutes at 800 °C as shown in Figure 5(b), the polarization curve showed a clear difference. The corrosion potential value of the 2.2Mo-2.2W specimen of which Mo was substituted with W was higher than that of the 3Mo specimen, -0.15 V (Ag/AgCl), showing a value of 0.07 V (Ag/AgCl), and its pitting potential value was also higher than that of the 3Mo specimen, 0.3V(Ag/AgCl), showing a value of 0.75 V (Ag/AgCl).

The most deadly form of corrosion in stainless steel is pitting corrosion. Critical pitting potential is the lowest potential which generates pitting corrosion, and, when the potential is increased even a little from this value, the current density rapidly increases generating pitting corrosion [18].

It can be said from this that, as to the characteristics of passive film seen on potentiodynamic polarization curves, the stability of the passive film on 2.2Mo-2.2W steel is superior to that on 3Mo steel as observed in the comparison between the pitting potentials of different steel grades.

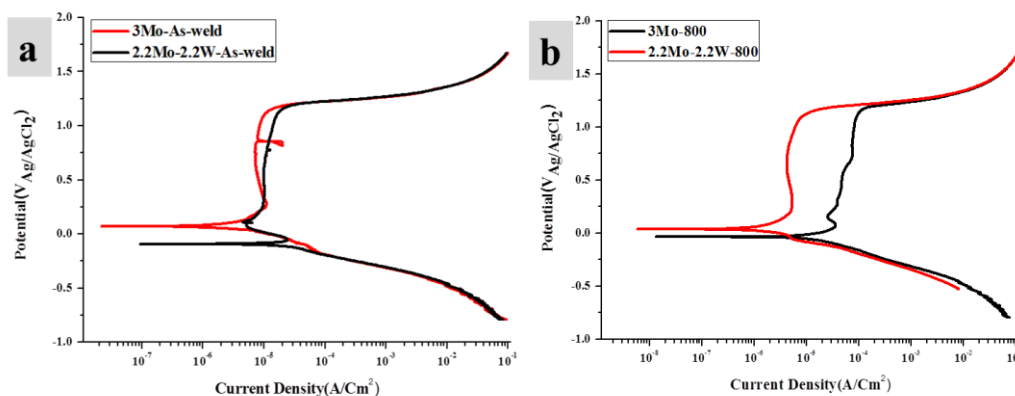


**Figure 5.** The Polarization Curves obtained from the Centre Region of Specimens in 3.5%NaCl : (a) 3Mo, (b) 2.2Mo-2.2W

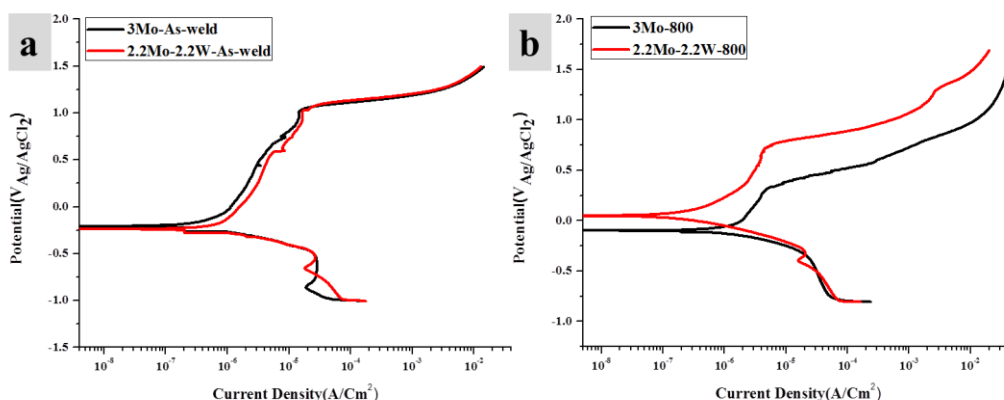


**Figure 6.** The Polarization Curves obtained from the Centre Region of Specimens in 1mol/L H<sub>2</sub>SO<sub>4</sub> : (a) 3Mo, (b) 2.2Mo-2.2W

Fig.6 shows the results of testing the anodic polarization behaviors of SDSS weld in 1M H<sub>2</sub>SO<sub>4</sub> solution of sulfuric acid environment. Though the two specimens in as weld state showed no big difference in the overall polarization behavior, the corrosion potential value of the 2.2Mo-2.2W specimen was higher than that of the 3Mo specimen, 0.18 V (Ag/AgCl), showing a value of 0.08 V (Ag/AgCl). Also, as in the chloride environment experimented earlier, the effect of W substitution appeared more apparently in the polarization behavior after the aging treatment. Though it took more time for the 2.2Mo-2.2W specimen to form the initial passive film, the stability of the passive film once formed was higher and the critical current density was lower than that of 3Mo specimen. Also, it could be seen that the pitting corrosion resistance of the 2.2Mo-2.2W specimen was superior to that of

the 3Mo specimen also in  $\text{H}_2\text{SO}_4$  solution as it had higher critical pitting potential (1.25 V), as if minor.

In the case Mo in DSS is partially substituted with W which makes an alloy containing Mo and W of a specific ratio, the pitting potential is known to improve together with delay in the speed of  $\sigma$  phase formation due to synergy effect of Mo and W [19, 20]. Though the synergy effect of Mo+W did not appear in the polarization test in as weld state, the corrosion characteristics in both chloride environment and sulfuric acid environment were improved due to (recommend to use 'because of', too frequently use 'due to') the Mo+W synergy effect in the polarization test after aging treatment.

### 3.3. Effect of the Secondary Phase Formation on Corrosion Resistance

Fig. 7(a) shows the results of analyzing the phase of the specimen aged for 30 minutes at 800 °C. Figure 7(b) shows the precipitation behaviors of  $\sigma$  phase which are in yellow color. During aging,  $\sigma$  precipitated along the  $\delta/\gamma$  grain boundary showing an almost continuous band form, and grew toward the inside of the grain as time passed by.

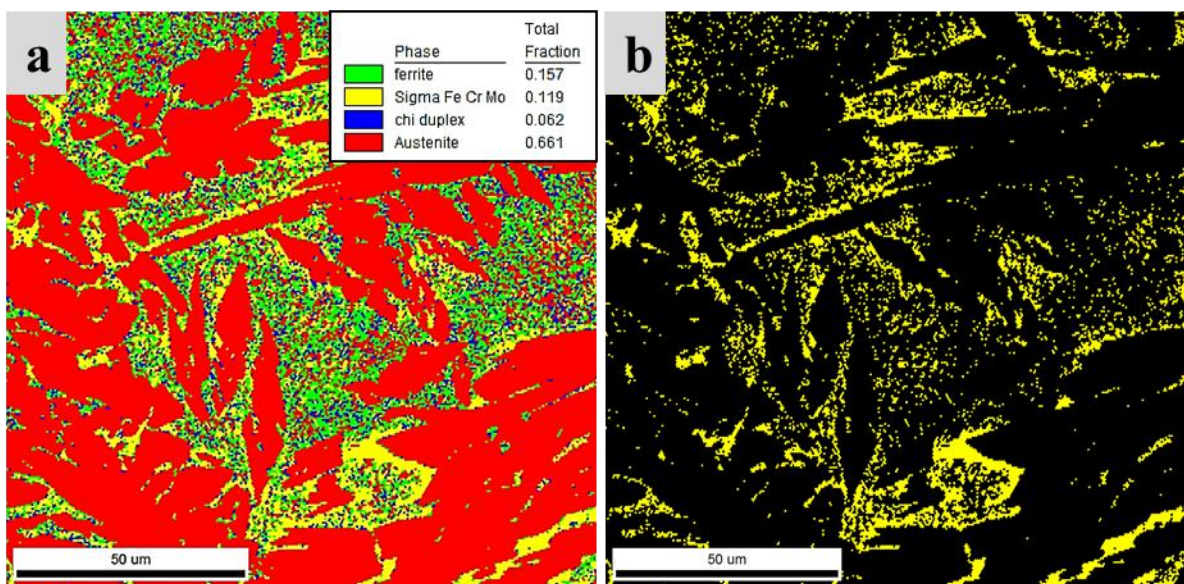


**Figure 7.** EBSD Phase Map. Color Scheme for Phase ID: Red- $\gamma$ -austenite, Green- $\delta$ -ferrite, Yellow-sigma Phase, Blue-chi Phase: (a) All Phases, (b) Sigma Phase

Fig. 8 shows the SEM structure of the specimen after the polarization test in the 3.5% NaCl solution. Pitting was generated along the  $\delta/\gamma$  grain boundary similarly to the  $\sigma$  phase precipitation behavior in Figure 7(b) above. That is to say, pitting corrosion intensively occurred from the area around the  $\sigma$  phase precipitated along the grain boundary, and the size of pit gradually increased as time passed by. It was because a Cr/Mo Depleted Zone lacking [21] Cr and Mo contents was formed around the  $\sigma$  phase because the precipitated  $\sigma$  came to contain more Cr and Mo elements than the matrix. According to the findings of Wilms [22] *et al.*, in the case of 24.01Cr-7.11Ni-3.89Mo-0.29N

DSS, pitting was generated in a Cr/Mo Depleted Zone around  $\sigma$  phase in aqueous solution of NaCl, and the  $\sigma$  phase itself remained as it was without being corroded. Such a fact can also be confirmed in Figure 8(b).

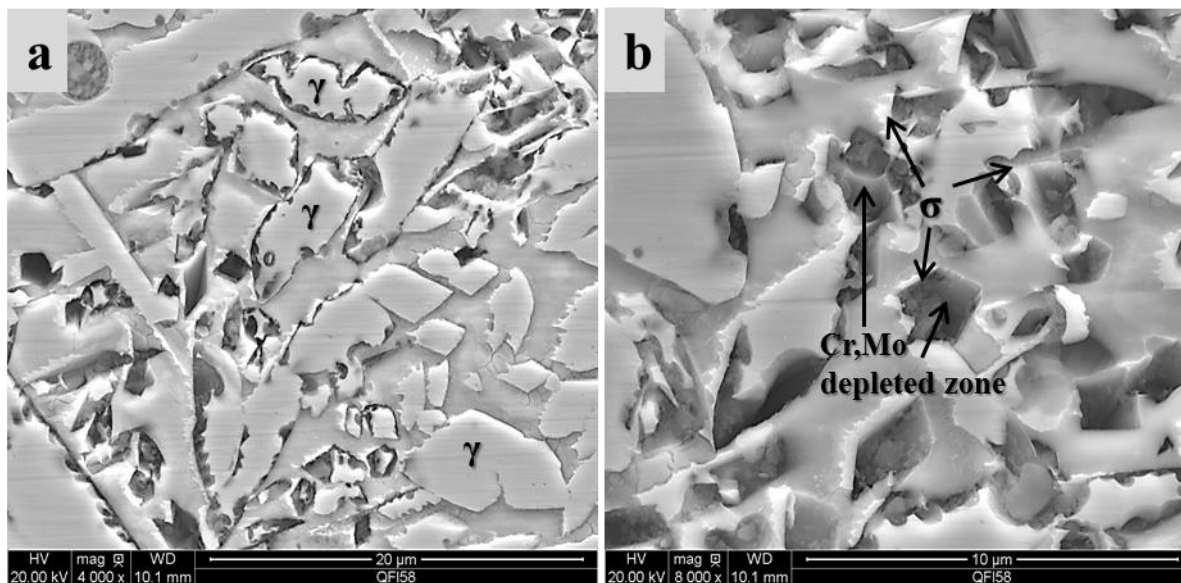


**Figure 8.** The Mechanism of Pitting Corrosion for Specimen aged at 800 °C

In general as well, existence of  $\sigma$  phase is known to reduce pitting resistance and crevice corrosion resistance capabilities. Therefore, in order to prevent deterioration of corrosion characteristics, precipitation of  $\sigma$  phase should be delayed and suppressed to the maximum.

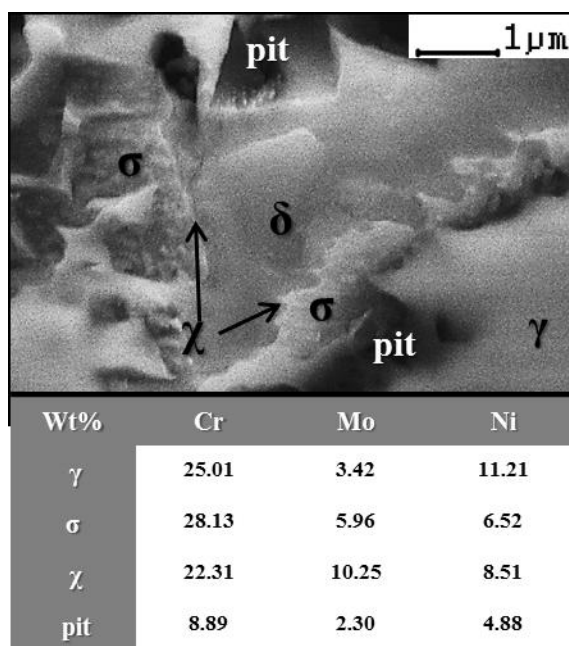


**Figure 9.** The Mechanism of Pitting Corrosion for Specimen aged at 800 °C

It was confirmed through the result of EBSD analysis conducted earlier that addition of W promotes precipitation of  $\chi$  phase and suppresses precipitation of  $\sigma$  phase. The corrosion resistance of the 2.2Mo-2.2W specimen was superior to that of the 3Mo specimen in spite of the precedent precipitation of  $\chi$  phase. The reason was that, though a Mo-depleted zone was formed around the precipitates as the Mo content of  $\chi$  phase was high as shown in Figure 9, a Cr-rich zone was formed around the precipitates as the Cr content was low. Accordingly, as Cr -richness offsets reduction in corrosion resistance caused by Mo depletion, the effect of  $\chi$  phase on reduction of potential is not significant [23].

In conclusion, reduction in pitting corrosion achieved by aging treatment is related to precipitation of  $\chi$  phase. That is to say, the corrosion characteristics of 2.2Mo-2.2W specimen can be said to have improved in comparison to those of the 3Mo specimen as formation of  $\sigma$  phase is reduced by substituting some of Mo elements with W elements, and, as a result, the degradation speed of pitting potential is also reduced by aging.

#### 4. CONCLUSIONS

FCAW was conducted for the welding materials produced adjusting the contents of Mo and W elements in alloys using the SDSS of class 40 pitting corrosion resistance index as the basic composition. By investigating the resulting microstructure and corrosion characteristics, the following conclusions are obtained:

- 1) The result of observing the microstructure showed that, as a result of substituting some of Mo with W, the fraction of  $\delta$ -ferrite increased and  $\gamma$  grew with a fixed directional property.
- 2) As a result of analyzing the specimen after aging it for 30 minutes at 800 °C, the  $\sigma$  phase precipitation in the specimen of which Mo was substituted with W was shown to be lower than that in the specimen containing only Mo by about 12 %.
- 3) As a result of the potentiodynamic polarization test, though no difference in the corrosion resistance was shown in the polarization test in as weld state, the specimen to which W was added showed corrosion resistance superior to that of the specimen to which only Mo was added in the polarization test conducted after aging treatment.
- 4) The result of analyzing the microstructure after the polarization test showed that pitting was generated in a Cr/Mo depleted zone round  $\sigma$  phase, and  $\sigma$  phase itself was not corroded.

#### ACKNOWLEDGEMENT

The present research was financially supported by the Ministry of Education, Science Technology (MEST) and National Research Foundation of Korea (NRF) through the Human Resource Training Project for Regional Innovation.

#### References

1. Robert N Gunn, *Duplex Stainless Steel*, Woodhead Publishing Ltd, Abinton, (1997)

2. Jerome Kruger, *Corros. Sci.*, 19 (1989) 149
3. M. Cohen, R. P Frankenthal, J. Kruger (Eds.), *Passivity of Metals*, The Electrochemical Society, Pennington, NJ (1978)
4. P. J. Grobner, *Metall. Trans.*, 4 (1973) 251
5. M. K. Miller, J. Bentley, *Mater. Sci. Technol.*, 3 (1990) 285
6. J. L. Ord, D. J. De Smet, *J. Electrochem. Soc.*, 123 (1976) 1876
7. C. Sunseri, S. Pizza, F. Di Quarto, *J. Electrochem. Soc.*, 137 (1990) 2411
8. K. Kondo, M. Ueda, K. Ogawa, M. Igarashi, *Proc. Conf. Innovation of stainless steel*, Florence, Italy, 2 (1993) 191
9. T. Huhtah, J. O. Nilsson, A. Wilson, P. Jonsson, *Proc. Conf. Duplex stainless steel '94*, Glasgow, Scotland, 1 (1994) 43
10. Y. H. Lee, K. T. Kim, Y. D. Lee, K. Y. Kim, *Mater. Sci. Technol.*, 8 (1998) 757
11. J. S. Kim, H. S. Kwon, *Corros.*, 55 (1999) 512
12. Y. S. Ahn, J. P. Kang, *Mater. Sci. Technol.*, 4 (2000) 382
13. A. Belfrouh, C. Masson, D. Vouagner, A. M. De Beudelievre, N. S. Prakash, J. P. Audouard, *Corros. Sci.*, 38 (1996) 1639
14. E.L. Brown, T.A. Whipple, G. Krauss, in: R.A. Lula (ed), *proceedings of conference on new developments in stainless steel technology*, ASM, Metals Park, OH, (1983)
15. H. M. Lee, S. M. Allen, M. Grujicic, *Metall. Trans. A*, 22 (1991) 2869
16. J. E. Shackelford, W. Alexander, J. S. Park, *Materials Science and Engineering Handbook*, CRC Press, Boca Raton, Florida, (1994)
17. Y. H. Lee, Y. D. Lee, K. T. Kim, K. Y. Kim, *Mater. Sci. Technol.*, 14 (1998) 757
18. J. O. Nilsson, A. Wilson, *Mater. Sci. Technol.*, 9 (1993) 545
19. B. W. Oh, J. I. Kim, S. W. Jeong, H. S. Kwon, Y. G. Kim, *Inter. Conf. on Processes and Materials Innovation Stainless Steel*, (1993) 59
20. H. Okamoto, K. Tsuda, S. Azuma, M. Ueda, K. Ogawa, M. Igarash, *Advanced Performance of 2% Tungsten Bearing Super Duplex Stainless Steel DP3W*, TWI, Glasgow Scotland (1994)
21. Y. S. Ahn, M. Kim, B. H. Jeong, *Mate. Sci. Technol*, 16 (2000) 382
22. M. E. Wilms, V. J. Gadgil, J. M. Krougman, F. P. Ijsseling, *Corros. Sci.*, 36 (1994) 871
23. C.J. Park, M.K. Ahn, H.S. Kwon, *J. Kor. Inst. Met. & Mater.*, 43 (2005) 595

© 2014 The Authors. Published by ESG ([www.electrochemsci.org](http://www.electrochemsci.org)). This article is an open access article distributed under the terms and conditions of the Creative Commons Attribution license (<http://creativecommons.org/licenses/by/4.0/>).